Atomistic simulation of the effect of temperature and pressure on point defect formation in $MgSiO_3$ perovskite and the stability of $CaSiO_3$ perovskite

2000 J. Phys.: Condens. Matter 12 8427

(http://iopscience.iop.org/0953-8984/12/39/306)

J. Phys.: Condens. Matter **12** (2000) 8427–8438. Printed in the UK PII: S0953-8984(00)15292-0

Atomistic simulation of the effect of temperature and pressure on point defect formation in $MgSiO_3$ perovskite and the stability of $CaSiO_3$ perovskite

G W Watson†§ , A Wall‡ and S C Parker‡

† Department of Chemistry, Trinity College, Dublin 2, Ireland

‡ Department of Chemistry, University of Bath, Claverton Down, Bath BA2 7AY, UK

E-mail: watsong@tcd.ie

Received 7 July 2000

Abstract. We present an atomistic simulation method for calculating the defect formation free energy and defect volume using lattice dynamics. The periodic simulation methods have been extended to allow charged systems with subtraction of defect–defect interactions to be studied routinely. This allows constant pressure minimization to be used rather than the more traditional constant volume method, allowing direct calculation of defect formation volumes and defect free energies or enthalpies rather than lattice energy.

We have applied this method to the calculation of enthalpies and volumes of vacancy and Schottky formation as a function of pressure and to the solution of Ca in the lower mantle mineral $MgSiO_3$ perovskite. The results indicate that as the pressure increases the defect volume of vacancy formation decreases and above approximately 50 GPa this decrease actually leads to a reduction in the enthalpy of formation rather than the expected increase as the pressure is increased further. The total Schottky enthalpy however continues to increase as a function of pressure although the rate of change of energy decreases with increasing pressure.

The solution of Ca with $MgSiO_3$ perovskite is shown to be very unfavourable and indicates that Ca will form its own $CaSiO_3$ perovskite phase within the conditions expected within the lower mantle. This result is important when considering the amount and location of trace elements such as Al within the mantle that have been shown to be preferentially located within $CaSiO_3$ perovskite rather than $MgSiO_3$ perovskite.

1. Introduction

The physical properties of ceramics and minerals including electronic and ionic conduction, diffusion and creep are highly dependent on the defects they contain including point defects, dislocations and grain boundaries (Catlow and Stoneham 1989, Catlow 1993, Sakaguchi *et al* 1992, Duffy 1986). Atomistic simulation has been used as a complementary tool for understanding the structure and properties of such defects due to the difficulty of probing them experimentally. These simulations have concentrated on point defects in ceramics (Tomlinson *et al* 1989, Islam and Baetzold 1992, Pryde *et al* 1995) although simulations have also been performed on surfaces (Watson *et al* 1996), grain boundaries (Harris *et al* 1996, 1999), hetero-interfaces (Sayle *et al* 1994) and dislocations (Watson *et al* 1999).

An understanding of the rheological behaviour of the Earth's lower mantle is required to model mantle dynamics. However, there is little information regarding the creep behaviour

§ Telephone. +353(0)1 608 1357. Fax. +353 (0)1 671 2826. http://www.ted.ie./Chemistry/People/Watson

0953-8984/00/398427+12$30.00

of lower mantle materials (primarily $(Mg, Fe)SiO_3$ perovskite and $(Mg, Fe)O$) at mantle conditions. Experiments of rheological behaviour on mantle materials are at present beyond the limits of technology due to the high temperatures and pressures required to stabilize $(Mg, Fe)SiO_3$ perovskite. Therefore alternative methods such as analogue studies have been used such as the creep experiments on the perovskites $CaTiO_3$ and $NaNbO_3$ performed by Wright *et al* (1992).

Solid state creep is a process that is be highly dependent on the ability of the ions to diffuse (Poirier 1985), which in turn depends on the free energy of defect formation and is thus amenable to the methods used to study defect formation in ceramics. Wall and Price (1989) calculated defect formation in $MgSiO_3$ perovskite while Wright and Price (1993) performed constant volume computer simulations on the formation and diffusion of defects in $SrTiO_3$, $CaTiO_3$ and $MgSiO_3$. We have also performed a previous study of defect formation in MgO (Mills *et al* 1991), which indicated that the defect formation volume is important and highly dependent on pressure, an effect not previously modelled and difficult to model in the constant volume methods previously employed.

Defect formation energies will also control the location of trace elements within the lower mantle. Revised estimates of the solar elemental abundance of calcium, indicate a higher value than previous determinations (Anderson and Bass 1984, Bass and Anderson 1984). It is thought to be present in the mantle and the most likely Ca bearing phase is $CaSiO_3$ perovskite (Ringwood and Major 1969, Tamai and Yagi 1989, Mao *et al* 1989). This phase may be an important deposit of trace elements within the mantle as recent studies have shown partitioning of rare earth elements to $CaSiO_3$ in preference to $MgSiO_3$ (Kato *et al* 1988). However, this relies on the assumption that $CaSiO_3$ exists as a separate phase within the lower mantle, and yet there is little information regarding its physical and chemical properties, largely due to the high pressure required to stabilize it. Some success has been achieved by Mao *et al* (1989) who studied the crystal structure up to 134 GPa. More recently Wang *et al* (1996) have studied the pressure–volume relationship of $CaSiO_3$ perovskite up to 13 GPa using more accurate methods.

Computer modelling of the $CaSiO_3$ perovskite phase was attempted in the late 1980s by Wolf and Bukowinski (1987) and by Hemley *et al* (1987) using the potential induced breathing (PIB) calculations. Neither of these obtained a reasonable equation of state (EOS) as highlighted by Sherman (1993), who performed an *ab initio* periodic Hartree–Fock study, which provided excellent agreement with the data of Mao *et al*.

Wentzcovitch *et al* (1995) and Warren *et al* (1998) have performed density functional theory (DFT) studies using the local density approximation (LDA), pseudopotentials and a plane wave basis set on both $MgSiO_3$ perovskite and $CaSiO_3$ perovskite. They found that $CaSiO_3$ perovskite is cubic from 0 to 150 GPa in agreement with Sherman. Stixrude *et al* (1996) and Chizmeshya *et al* (1996) employed the linear augmented plane wave (LAPW) technique and the LDA to calculate both the EOS and the phonon frequencies. Both of these studies, in contrast to both the above calculations, indicate that the cubic phase of $CaSiO_3$ perovskite will be dynamically unstable at all pressures. $CaSiO_3$ perovskite cannot be stabilized at ambient pressures (Wang and Weidner 1994) and so dynamical instabilities at low pressure may be expected. Wang *et al* (1996) have examined the phase boundary between $Ca_2SiO_4 + CaSi_2O_5$ and $CaSiO_3$ perovskite indicating a phase boundary along the line 11 GPa, 1500 K and 9 GPa, 600 K. At higher temperature and pressures $CaSiO_3$ perovskite was found to be cubic in agreement with the studies of Wang and Weidner (1994) and Liu and Ringwood (1975).

This paper will present an atomistic simulation method for studying defect formation as a function of temperature and pressure. We have used this technique to study the thermodynamics of defect formation in $MgSiO_3$ perovskite which will be a vital step in the mechanism of

Table 1. Parameters of the potential model.

Species	Charge	ij	A_{ij} (eV)	r_{ij} (Å)	C_{ij} (eV Å^6)
Mg	+2	Mg–O_{shell}	1 233.8032	0.294 53	0.0
Ca	+2	Ca–O_{shell}	1 090.4	0.340 0	0.0
Si	+4	Si–O_{shell}	1 383.735	0.320 52	10.661 58
O_{shell}	−2.848	O_{shell}–O_{shell}	22 764.0	0.149 0	27.88
O_{core}	+0.848	O_{core}–O_{shell}	Core-shell spring constant $k = 74.92$ eV Å^2		

O_{shell}–Si–O_{shell} three body spring constant $k = 2.097\,24$ eV rad^{-1}, short range cutoff 12 Å.

ion transport important in such mantle processes as convection, ionic conductivity, thermal conductivity and creep but also has direct applications in the calculation of defect free energies in ceramics. We will focus on the formation of Schottky and pseudo-Schottky defects in $MgSiO_3$ and the inclusion of calcium in the lower mantle, either dissolved within $MgSiO_3$ or as a separate $CaSiO_3$ perovskite phase.

2. Atomistic simulation techniques

The atomistic simulation method employed is based on the Born model of solids in which the system is modelled by summation of individual interactions defined by an interatomic potential. These interactions include coulombic and two body, short range interactions, to model electron cloud repulsion and van der Waals attractions. In addition a three body term is used to infer directionality on the two body bonding around the Si and the shell model of Dick and Overhauser (1959) describes the electronic polarizability of the oxygen ions.

The potential parameters used for the $MgSiO_3$ (PVTHB1) are shown in table 1 and were developed by Wall and Price (1989) to model $MgSiO_3$ perovskite. In addition a potential model was required to allow the calculation of calcium defects, the potential parameters for which are also included in table 1 and were derived by Lewis and Catlow (1984).

The simulations were performed with the atomistic free energy minimization code PARAPOCS (phonon assisted relaxation applied to the prediction of crystal structure) (Parker and Price 1989, Watson *et al* 1997). Periodic boundary conditions are assumed and the cell relaxed to minimum free energy, given by

$$G = U_{latt} + PV + U_{vib} - TS_{vib}$$

where U_{latt} is the internal lattice energy, P is the pressure, V is the cell volume, U_{vib} is the vibrational energy (including zero point energy), T is the temperature and S_{vib} is the vibrational entropy.

In a previous study (Mills *et al* 1991) we observed problems due to defect–defect interactions in the calculations arising from the periodic boundary conditions employed. The sum of the coulombic energy required a neutral cell; this coupled with the periodic boundary conditions meant that each cell contained two defects, to maintain charge neutrality, and that these interacted with each other and their images in the periodic summation. To reduce these effects a number of program developments have been made to allow the simulation of single charged point defects with subtraction of defect–defect interactions allowing simulation close to infinite dilution to be obtained.

The Ewald method, which is used to sum the coulombic terms, assumes that the cell is charge neutral; however a small modification allows charged cells to be considered. This is treated by assuming there is a counter-charge which is distributed evenly throughout the cell

Table 2. Defect energy, charge correction and defect–defect interaction energy as a function of supercell size.

Cell size				
Number of cells	Number of ions (cores)	V(Mg) (eV)	Coulomb correction (eV)	Defect–defect interaction (eV)
1 1 1	20	24.82	1.94	−1.04
1 1 2	40	25.31	1.22	−0.40
1 2 1	40	25.43	1.22	−0.74
2 1 1	40	25.56	1.22	−0.75
2 2 2	160	25.91	0.49	−0.52
3 2 2	240	25.97	0.37	−0.45
3 3 3	540	26.00	0.22	−0.35
Cascade	436[a]	26.07		

[a] Number of ions (cores) in region 1.

and is the $g = 0$ term for the reciprocal space summation (Leslie and Gillan 1985) given by

$$-\frac{\pi Q^2}{2V\eta}$$

where Q is the total charge on the cell, V is the cell volume, and η is the Gaussian half width used in the Ewald sum. In addition the coulombic interaction energy from defect–defect interactions can be calculated (see Allan *et al* 1989) as

$$\sum_{i,j}^{defects''} \left(\frac{q_i q_j}{2\underline{r}_{ij} \cdot \underline{\underline{\varepsilon}}_R} \right)$$

where $''$ indicates the summation does not include pairs of defects within the unit cell, $\underline{r}_{ij}$ is the distance between defects i and j and $\underline{\underline{\varepsilon}}_R$ is the static dielectric constant matrix.

The extensions used in this study are, firstly, the use of the vector product of the distance between defects and the static dielectric matrix allowing symmetries other than cubic the be used, and, secondly, that these interactions are calculated during the simulation and not applied retrospectively (Allan *et al* 1989). The forces due to defect–defect interactions are also calculated and subtracted and are therefore excluded from affecting the final configuration and energy. Defect clusters can still be considered as the interactions are only subtracted between until cells but in this study we have only considered isolated defects.

The method used to remove defect–defect interactions is not perfect. It only subtracts coulombic interactions and thus short range effects are still included. In addition if the defect is too close to its images the forces and thus the resulting energy and configuration will be altered by interaction with the perturbed lattice around the defect image. We have thus studied the effect of supercell size on the simplest defect in $MgSiO_3$ perovskite (magnesium vacancy) to assess the size of supercell required for further calculation. The energy of the magnesium vacancy was calculated (neglecting temperature) with increasing cell size up to a $3 \times 3 \times 3$ supercell of 540 atoms and are compared to the same defect calculated at infinite dilution using the CASCADE program (Leslie 1981). CASCADE, which has previously been used to study point defects in perovskite (Wall and Price 1989, Wright and Price 1993), uses a two region Mott–Littleton type approach (Catlow 1989) at constant volume and thus for the purposes of the test the volume of the supercell was held fixed. Table 2 shows the variation in the vacancy energy as a function of supercell size and also includes the two correction terms, which show that they are not insignificant although they do cancel each other out to some degree. The results show that the defect energy tends toward the CASCADE energy with increasing supercell size

Table 3. Vacancy formation enthalpies as a function of pressure.

Pressure (GPa)	V(Mg) (kJ mol^{-1})	V(Ox) (kJ mol^{-1})	V(Si) (kJ mol^{-1})
0	2501	2277	9079
6	2507	2276	9121
10	2509	2274	9145
30	2510	2269	9223
50	2499	2252	9275
80	2458	2216	9276
100	2419	2188	9250
150	2289	2094	9098

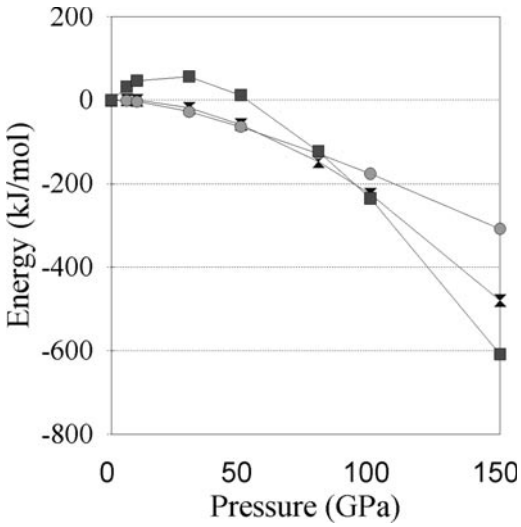

Figure 1. Variation in $P\delta V$ of vacancy formation as a function of pressure for silicon (square), magnesium (hourglass) and oxygen (circle).

with the largest ($3 \times 3 \times 3$) being the closest. Due to the large size of this supercell and to allow as many calculations to be performed as possible the supercell of size ($2 \times 2 \times 2$) was chosen as it represents a manageable size while giving good accuracy.

3. Vacancy formation energies and volume

In our previous study of MgO (Mills *et al* 1991) the defect formation energy was only weakly dependent on temperature while being strongly dependent on pressure; therefore we have neglected the temperature component of the free energy, and performed static calculations allowing more extensive studies to be conducted.

In the intrinsic defect region the concentration of impurities is low and defect processes are dominated by the defect formation energy. We have therefore calculated the defect energies as a function of pressure from 0 to 150 GPa, shown in table 3. We have only included a single oxygen vacancy energy because, although $MgSiO_3$'s orthorhombic nature gives rise to two distinct oxygens, the vacancy formation energies are within 1 kJ mol^{-1}.

The oxygen vacancy has the lowest enthalpy of formation across the whole pressure range and is made up of two components, the lattice energy and the PV terms. The total defect formation energy decreases with increasing pressure. This effect is due to a reduction in the

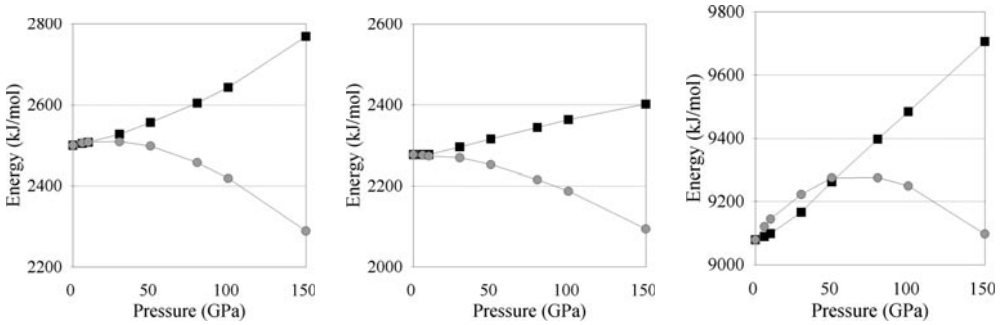

(a) (b) (c)

Figure 2. Variation in energy (square) and enthalpy (circle) as a function of pressure for (a) oxygen, (b) magnesium and (c) silicon vacancy formation.

activation volume of defect formation as a function of pressure (figure 1), which outweighs the increase in lattice energy (figure 2(a)). This is an important point as previous calculations (Wall and Price 1989, Wright and Price 1993) have used a constant volume approach which cannot take into account the volume term shown in figure 1.

The same effect can be seen in the magnesium vacancy. This is slightly less energetically favourable than oxygen (table 3) and shows a positive δV at low pressure, causing an increase in the enthalpy of defect formation over the lattice energy of defect formation. However, at high pressure similar to the lower mantle, the δV term becomes negative (figure 1) and the enthalpy of defect formation reduces as a function of pressure (figure 2(b)). This change is due to the high hydrostatic pressure overcoming the electrostatic repulsion set up by the magnesium vacancy and can be seen by the changes in bond lengths. At 0 GPa the Mg–O bond length is 2.20 Å and on introducing a vacancy the distance between the vacant site and an adjacent oxygen increases to 2.37 Å as a result of electrostatic repulsion between the vacancy (effective charge -2) and the oxygen ions (charge -2). At 100 GPa the effect is reversed. The Mg–O bond distance is 2.04 Å and the vacancy–oxygen distance is 2.00 Å, indicating that at high pressure it is the short range component of the interaction which dominates the repulsion.

The most unexpected result is that of the enthalpy of vacancy formation for the silicon. This shows a high formation enthalpy (9079 kJ mol^{-1} at 0 GPa) and increases with pressure due to both an increase in lattice energy (figure 2) and a positive volume change (figure 1) reaching (9275 kJ mol^{-1} at 50 GPa). However, at around 70 GPa the δV rapidly changes to a negative value, causing the enthalpy of vacancy formation to rapidly reduce, reaching 9098 kJ mol^{-1} at 150 GPa. The effect of pressure on the enthalpy is therefore dominated by the lattice energy at low pressure (figure 2(c)) and the $P\delta V$ term at high pressure (figure 1).

The silicon vacancy is potentially the hardest to calculate due to the large charge and volume changes which accompany vacancy formation. Due to these effects the silicon vacancy will be the least accurate and will potentially require larger supercells for accurate results. We have therefore performed silicon vacancy calculations for a $3 \times 3 \times 3$ supercell (540 cores) to check the observed reduction in the enthalpy of formation. These show good agreement with the smaller supercell (9094 kJ mol^{-1} at 0 GPa, 9303 kJ mol^{-1} at 50 GPa, 9297 kJ mol^{-1} at 100 GPa and 9156 kJ mol^{-1} at 150 GPa) with the closest agreement at 0 GPa where the cell volume, and thus the defect–defect distance, is greatest.

4. Schottky defects in $MgSiO_3$

Enthalpies are calculated for isolated defects and the Schottky energies simply obtained by summation, assuming the ions are moved to the surface, i.e.

$$\Delta H_{f(MgSiO_3)} = (E' - E)_{Mg} + (E' - E)_{Si} + 3(E' - E)_O + E''_{(MgSiO_3)}$$

where E represents the enthalpy (lattice energy and PV terms) of the pure system, E' indicates the enthalpy of the defective lattice and E'' is the energy of the removed unit. In addition the so called pseudo-Schottky defects created by removing a charge neutral but not necessarily stoichiometric unit have been calculated, i.e.

$$\Delta H_{f(MgO)} = (E' - E)_{Mg} + (E' - E)_O + E''_{(MgO)}$$
$$\Delta H_{f(SiO_2)} = (E' - E)_{Si} + 2(E' - E)_O + E''_{(SiO_2)}.$$

The enthalpy for the removed phase is obtained by performing calculations using the same potentials. For MgO this is periclase but for SiO_2 this would involve calculation of α-quartz/coesite/stishovite depending on the pressure. However, since $MgSiO_3$ perovskite is a high pressure phase we have used is our calculations the high pressure phase of SiO_2 (stishovite).

The variation in the lattice energy component of the Schottky defect energy is shown in figure 3(a). This indicates that, as in previous calculations employing the embedded atom approach (Wall and Price 1989, Wright and Price 1993), the Schottky formation lattice energy increases as a function of pressure. The most stable defect is the MgO pseudo-Schottky which at 345.7 kJ mol^{-1} is 62.7 kJ mol^{-1} more stable than the full Schottky and 132.8 kJ mol^{-1} more stable than the SiO_2 pseudo-Schottky at 0 GPa. The formation energy rises to 505.4 kJ mol^{-1} at 100 GPa (103.6 and 201.8 kJ mol^{-1} more stable than the full Schottky and SiO_2 pseudo-Schottky, respectively) and 633.5 kJ mol^{-1} at 150 GPa (111.6 and 215.9 kJ mol^{-1} more stable). This compares with the recent calculations of Wright and Price (1993) in which the MgO Schottky has a defect formation energy of 353.6 kJ mol^{-1} at 0 GPa (45.4 kJ mol^{-1} more stable than the full Schottky and 115.9 kJ mol^{-1} more stable that the SiO_2 pseudo-Schottky) and 635.6 kJ mol^{-1} at 125 GPa (205.1 and 339.4 kJ mol^{-1} more stable).

The effect of including the PV term in the energy of the Schottky is illustrated by Schottky formation enthalpy (figure 3(b)). This shows that due to a positive defect volume (figure 3(c)) the Schottky formation enthalpy is more positive that the lattice energy component. At low pressure the Schottky enthalpy increases rapidly above the lattice energy as a function of pressure. This is caused by a rapid increase in the Schottky PV term (figure 3(d)) at low pressure caused by the large Schottky formation volume (figure 3(c)). The effect does not increase rapidly beyond 50 GPa because the increasing pressure causes a rapid reduction in the formation volume, which reduces the effect of increasing pressure on the PV term. This effect is so marked that the PV contribution at 150 GPa is less than that at 100 GPa (figure 3(c)) as result of the reduced formation volume (figure 3(d)). This effect is more pronounced for the large Schottky and SiO_2 pseudo-Schottky leading to a reduction in the difference in energy between these and the MgO pseudo-Schottky from 111.6 and 215.9 kJ mol^{-1} using the lattice energy to 102.9 and 208.9 kJ mol^{-1} once the PV term has been considered. This effect was not observed in previous simulation studies as they considered constant volume simulations.

In summary the inclusion of the PV term in the defect formation energies leads to a different picture of the pressure dependence. At low pressure the lattice energy increases gradually while the PV term causes the enthalpy to increase more rapidly. At high pressure the lattice energy increases rapidly while the reduction in the defect volume causes the enthalpy to remain almost constant. Clearly the inclusion of the volume change and associated PV energy term is very important in calculating the defect formation energy.

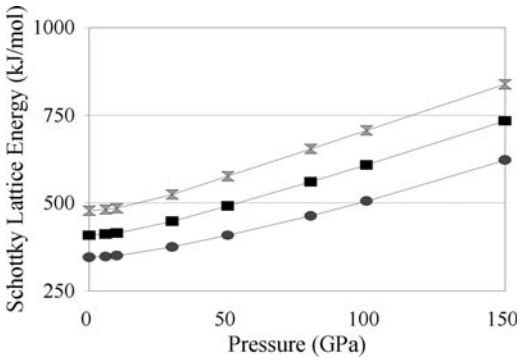

(a)

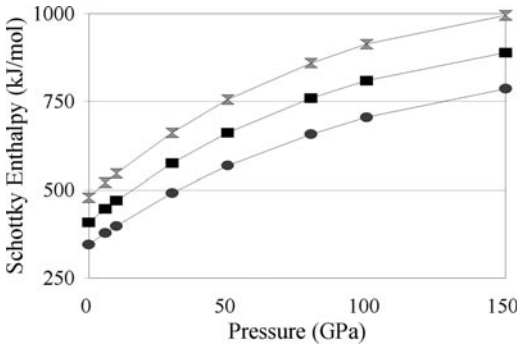

(b)

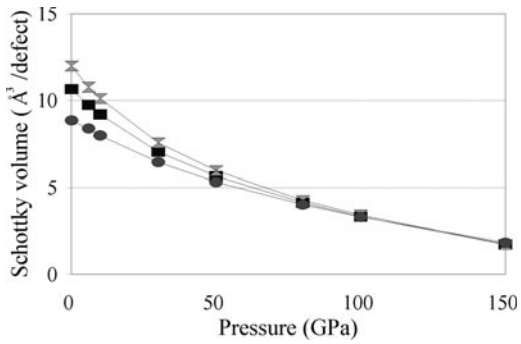

(c)

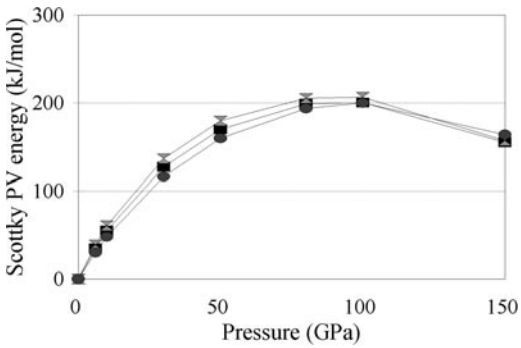

(d)

Figure 3. Effect of pressure on (a) the Schottky formation lattice energy (b) the Schottky formation enthalpy, (c) the Schottky formation volume and (d) the Schottky formation PV term.

Table 4. Predicted lattice parameter and bulk modulus for $CaSiO_3$ perovskite with the observed lattice parameter of Mao *et al* (1989) and bulk modulus obtained from Mao's Birch–Murnaghan equation of state ($K_0 = 281$, $K_0' = 4$).

	Mao *et al* (1989)		Predicted values	
Pressure	Lattice parameter (Å)	Bulk modulus (GPa)	Lattice parameter (Å)	Bulk modulus (GPa)
0	3.566	281	3.662	289.5
7.6	3.533	312	3.631	317.2
12.6	3.514	330	3.612	335.0
16	3.506	344	3.560	346.9
21.5	3.490	364	3.581	365.8
28.4	3.467	390	3.559	389.2
39.6	3.428	431	3.526	426.4
52	3.404	476	3.493	466.6
85.7	3.326	594	3.418	571.9
117.5	3.277	702	3.360	667.4
150		810	3.309	762.1

5. Calcium partitioning within the lower mantle

Simulations have been performed for cubic $CaSiO_3$ perovskite up to 150 GPa at 300 K, with the predicted lattice parameter and bulk modulus compared with Mao *et al* (1989) in table 4. The pressure dependence of the structure is modelled well with the bulk modulus at very high pressure deviating slightly from that of Mao. In our calculations $CaSiO_3$ perovskite is dynamically stable down to 0 GPa in agreement with the calculations of Sherman (1993), Wentzcovitch *et al* (1995) and Warren *et al* (1998). This indicates that the cubic form is more stable than a distorted perovskite (such as that adopted by $MgSiO_3$ perovskite) although it does not indicate that we would predict the structure to be observed at 0 GPa.

In addition to the tests on the P–V relationship of $CaSiO_3$, we have performed simulations on a range of materials, MgO, CaO, diopside, wollastonite and enstatite to verify the accuracy of the potential models. We are primarily interested in calculating the effect of temperature and pressure on the defect substitution energy of Ca within $MgSiO_3$ perovskite. We have therefore tested the potentials for the energetics of forming mixed Ca/Mg phases by using the lattice energies to calculate two reaction energies,

$$2MgSiO_3 + CaO \rightarrow MgCaSi_2O_6 + MgO \tag{1}$$

and

$$MgCaSi_2O_6 \rightarrow MgSiO_3 + CaSiO_3. \tag{2}$$

By comparing the reaction energies from the calculated lattice energies with those of the experimental heats of formation we can estimate the magnitude of the errors we would expect in calculating Ca solution in $MgSiO_3$ perovskite. Using the lattice energies the reaction energy for reaction (1) gave a reaction energy of -99.6 kJ mol^{-1} while using the heats of formation from Berman (1988) gave rise to -74.9 kJ mol^{-1}. For reaction (2) the agreement is even better with the lattice energies giving +20.8 kJ mol^{-1} and the heats of formation +21.5 kJ mol^{-1}. These calculations give us confidence in the ability of the potential model to predict solution energies of Ca within magnesium silicates and thus we have confidence in using it to predict solution energies in $MgSiO_3$ pv.

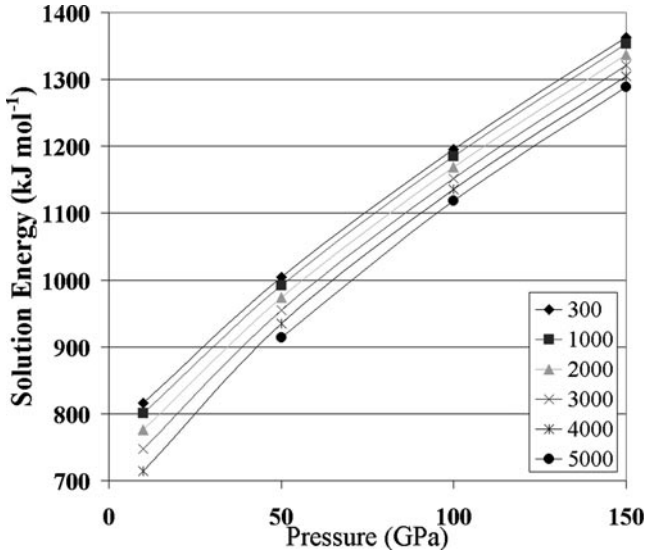

Figure 4. The effect of pressure and temperature on the substitution energy of Ca in $MgSiO_3$ perovskite.

To calculate whether Ca will dissolve in $MgSiO_3$ or form its own phase we use the mass action equation

$$\exp\left(\frac{-\Delta G}{RT}\right) = \frac{\lfloor \mathrm{Ca}_{MgSiO_3} \rfloor}{\lfloor \mathrm{Ca}_{CaSiO_3} \rfloor}$$

where ΔG is the difference in substitutional energies for Ca in $MgSiO_3$ and $CaSiO_3$, the latter of which in this case is zero and is therefore the solution energy of Ca in $MgSiO_3$.

The solution free energies have been calculated as a function of both temperature (300–5000 K) and pressure (10–150 GPa) and are shown in figure 4. At 300 K and 10 GPa the solution energy is 816 kJ mol^{-1} and rises steadily as a function of pressure, reaching 1362 kJ mol^{-1}. At all temperatures the same trend is observed, with an increase of around 600 kJ mol^{-1} over the pressure range. For a given pressure the temperature reduces the free energy of substitution. At 10 GPa the simulation at 5000 K produced imaginary frequencies, indicating that the harmonic approximation had broken down. Between 300 K and 4000 K the formation free energy reduces from 816 kJ mol^{-1} to 714 kJ mol^{-1}. Similar trends with temperature are observed at all pressures.

The effect of pressure was thus to increase the free energy of solution while temperature reduced the free energy. Using the mass action equation we can calculate the thermodynamic partition coefficient of Ca within the $MgSiO_3$ perovskite phase as a function of temperature and pressure. However, the substitution energies are so large that effectively all of the Ca will prefer to form its own phase, indicating that $CaSiO_3$ perovskite will be present within the lower mantle.

Experimental observations generally show that there is a very limited solubility of Ca in $MgSiO_3$ (Irifune 1994, Ahmen-Zaid and Madon 1995) in agreement with our calculations; however Liu (1987) reports a solid solution between $CaSiO_3$ and $CaMgSi_2O_6$. It is has been suggested that Liu's results may have arisen from the formation of metastable quench products from glassy starting materials (Mao *et al* 1989). Irifune (1994) showed that at pressures above 24 GPa pyrolite transformed with the majority of the Ca forming $CaSiO_3$ perovskite. Ahmen-

Zaid and Madon (1995) also found that at pressures between 40 and 50 GPa that $CaSiO_3$ perovskite was the main Ca bearing mineral.

These experimental observations and simulation results, which predict that $CaSiO_3$ perovskite will be stable throughout the lower mantle, indicate with the observation of preferential uptake of trace elements that the material may be a store for these trace elements within the lower mantle.

6. Conclusions

We have illustrated a method in which the errors associated with the overall charge of the cell and defect–defect coulombic interactions within a periodic atomistic calculation can be removed during the simulations rather than *post hoc*. This method allows the calculation of both the free energy and volume of defect formation. We have demonstrated this method by calculating the enthalpy of vacancy formation and Schottky formation in $MgSiO_3$ perovskite. The results indicate that pressure has a very large effect on the defect volume and that at high pressure (>50 GPa) the reduction in the volume of the defects is so large that it leads to a reduction in the enthalpy of formation.

In addition we have calculated the solution energy of Ca in $MgSiO_3$ perovskite, which clearly indicates that Ca will prefer to form is own $CaSiO_3$ perovskite phase. This is important because recent experiments have indicated that trace elements preferentially dissolve in $CaSiO_3$ perovskite, which would make it a source for such elements within the lower mantle. Further calculations are planned to investigate the partitioning of trace elements between $CaSiO_3$ and $MgSiO_3$ perovskites at mantle conditions.

Acknowledgments

We would like to thank the EPSRC and NERC for funding.

References

Ahmen-Zaid I and Madon M 1995 *Earth Planet. Sci. Lett.* **129** 233
Allan N L, Mackrodt W C and Leslie M 1989 *Adv. Ceram.* **23** 257
Anderson D L and Bass J D 1984 *Geophys. Res. Lett.* **11** 637
Bass J D and Anderson D L 1984 *Geophys. Res. Lett.* **11** 237
Berman R G 1988 *J. Petrol.* **29** 445
Catlow C R A 1989 *J. Chem. Soc. Faraday Trans.* II **85** 335
——1993 *Defects and Disorder in Crystalline and Amorphous Solids* (Dordrecht:Kluwer) (NATO ASI Series C 418)
Catlow C R A and Stoneham A M (eds) 1989 *J. Chem. Soc. Faraday Trans.* II **85** part 5
Chizmeshya A V G, Wolf G H and McMillan P F 1996 *Geophys. Res. Lett.* **23** 2725
Dick B G and Overhauser A W 1958 *Phys. Rev.* B **8** 5747
Duffy D M 1986 *J. Phys. C: Solid State Phys.* **19** 4394
Harris D J, Watson G W and Parker S C 1996 *Phil. Mag.* A **74** 407
——1999 *Am. Mineral.* **84** 138
Hemley R J, Jackson L and Gordon R G 1987 *Phys. Chem. Mineral.* **14** 2
Islam M S and Baetzold R C 1992 *J. Phys. Chem. Solids* **53** 1105
Irifune T 1994 *Nature* **370** 121
Kato T, Ringwood A E and Irifune T 1988 *Earth Planet. Sci. Lett.* **89** 123
Leslie M 1981 *EPSRC Daresbury Laboratory Technical Memorandum* DL/SCI-TM31T
Leslie M and Gillan M J 1985 *J. Phys. C: Solid State Phys.* **18** 973
Lewis G V and Catlow C R A 1985 *J. Phys. C: Solid State Phys.* **18** 1149
Liu L G 1987 *Geophys. Res. Lett.* **14** 1079
Liu L G and Ringwood A E 1975 *Earth Planet. Sci. Lett.* **14** 1079

Mao H K, Chem L C, Hemley R J, Jephcoat A P and Yu Y 1989 *J. Geophys. Res.* **94** 17 889
Mills D R, Parker S C and Wall W 1991 *Phil. Mag.* A **64** 1
Parker S C and Price G D 1989 *Adv. Solid State Chem.* **1** 295–7
Poirier J P 1985 *Creep of Crystals* (Cambridge: Cambridge University Press)
Pryde A K, Vyas S, Grimes R W, Gardner J A and Wang R 1995 *Phys. Rev.* B **52** 13 214
Ringwood A E and Major A 1971 *Earth Planet. Sci. Lett.* **12** 411
Sakaguchi I, Yurimoto H and Sueno S 1992 *Solid State Commun.* **84** 889
Sayle D C, Sayle T X T, Parker S C, Catlow C R A and Harding J H 1994 *Phys. Rev.* B **50** 14 498
Sherman D M 1993 *J. Geophys. Res.* **98** 19 795
Stixrude L, Cohen R E, Yu R C and Krakauer H 1996 *Am. Mineral.* **81** 1293
Tamai H and Yagi T 1989 *Phys. Earth and Planet Inter.* **54** 370–377
Tomlinson S M, Freeman C M, Carlow C R A, Donnerberg H and Leslie M 1989 *J. Chem. Soc. Faraday Trans.* II **85** 367
Wall A and Price G D 1989. Defects and diffusion in $MgSiO_3$ perovskite *Proc. Perovskite Chapman Conf.* ed A Navrotsky and D J Weidner (Washington, DC: American Geophysical Union)
Wang Y B and Weidner D J 1994 *Geophys. Res. Lett.* **21** 895
Wang Y, Weidner D J and Guyot F 1996 *J. Geophys. Res.* **101** 661
Warren M C, Ackland G J, Karki B B, Clark S J 1998 *Mineral. Mag.* **62** 585
Watson G W, Kelsey E T, de Leeuw N H, Harris D J and Parker S C 1996 *J. Chem. Soc. Faraday Trans.* **92** 433
Watson G W, Kelsey E T and Parker S C 1999 *Phil. Mag.* A **79** 527
Watson G W, Tschaufeser T, Wall A, Jackson R A and Parker S C 1997 Modelling the crystal structures of inorganic solids using lattice energy and free-energy minimisation *Computer Modelling in Inorganic Crystallography* ed C R A Catlow (New York: Academic)
Wentzcovitch R M, Ross N L and Price G D 1995 *Phys. Earth Planet. Interiors* **90** 101
Wolf G and Bukowinski M 1987 Theoretical study of the structural properties and equations of state of $MgSiO_3$ and $CaSiO_3$ perovskite: implications for lower mantle composition *High Pressure Research in Mineral Physics (Geophys. Monogr. Ser. 39)* ed M H Manghani and T Syono (Washington, DC: American Geophysical Union) pp 313–31
Wright K and Price G D 1993 *J. Geophys. Res.* **98** 22 245
Wright K, Price G D and Poirier J P 1992 *Phys. Earth Planet. Int.* **74** 9–22